Article

pubs.acs.org/Biomac

Π−Π Stacking Increases the Stability and Loading Capacity of Thermosensitive Polymeric Micelles for Chemotherapeutic Drugs

Yang Shi,[†] Mies J. van Steenbergen,[†] Erik A. Teunissen,[†] Luís Novo,[†] Sabine Gradmann,[‡] Marc Baldus,[‡] Cornelus F. van Nostrum,[†] and Wim E. Hennink*[,†]

[†]Department of Pharmaceutics, Utrecht Institute for Pharmaceutical Sciences (UIPS), Utrecht University, Universiteitsweg 99, P.O. Box 80082, 3508 TB Utrecht, The Netherlands

[‡]Bijvoet Center for Biomolecular Research, Utrecht University, Padualaan 8, 3584 CH Utrecht, The Netherlands

Supporting Information

ABSTRACT: Thermosensitive amphiphilic block copolymers self-assemble into micelles above their lower critical solution temperature in water, however, the micelles generally display mediocre physical stability. To stabilize such micelles and increase their loading capacity for chemotherapeutic drugs, block copolymers with novel aromatic monomers were synthesized by free radical polymerization of *N*-(2-benzoyloxypropyl methacrylamide (HPMAm-Bz) or the corresponding naphthoyl analogue (HPMAm-Nt), with *N*-(2-hydroxypropyl) methacrylamide monolactate, using a polyethylene glycol based macroinitiator. The critical micelle temperatures and critical micelle concentrations decreased with increasing the HPMAm-Bz/Nt content. The micelles of 30−50 nm were prepared by heating the polymer aqueous solutions from 0 to 50 °C and were colloidally stable for at least 48 h at pH 7.4 and 37 °C. Paclitaxel and docetaxel encapsulation was performed by mixing drug solutions in ethanol with polymer aqueous solutions and heating from 0 to 50 °C. The micelles had a drug loading capacity up to 34 wt % for docetaxel, which is among the highest loadings reported for polymeric micelles, with loaded micelle sizes ranging from 60 to 80 nm. The micelles without aromatic groups almost completely released loaded paclitaxel in 10 days, whereas the HPMAm-Bz/Nt containing micelles released 50% of the paclitaxel at the same time, which showed a better retention for the drug of the latter micelles. ^{1}H solid-state NMR spectroscopy data are compatible with $\pi-\pi$ stacking between aromatic groups. The empty micelles demonstrated good cytocompatibility, and paclitaxel-loaded micelles showed high cytotoxicity to tumor cells. In conclusion, the $\pi-\pi$ stacking effect introduced by aromatic groups increases the stability and loading capacity of polymeric micelles.

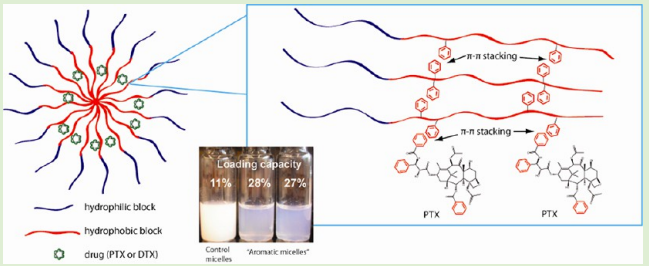

1. INTRODUCTION

During the past decades, polymeric micelles formed from amphiphilic block copolymers have been extensively investigated as drug delivery systems, particularly for the targeted delivery of hydrophobic drugs.[1−3] Polymeric micelles are characterized by a size normally below 100 nm and a good accommodation for poorly water-soluble drugs. Their hydrophilic corona, mostly consisting of poly(ethylene glycol) (PEG), endows them with a stealth surface, likely as a result of a low protein binding to the particles in the blood circulation.[4−6] Further, multifunctions can be introduced including decorating the surface with targeting ligands and incorporation of imaging agents.[7−11]

Among different types of amphiphilic block copolymers, thermosensitive block copolymers are receiving increased interest for the preparation of micelles,[12,13] hydrogels[14,15] and to coat liposomes.[16] Thermosensitive copolymers, which have a thermosensitive and a permanently hydrophilic block, form micelles above the critical micelle temperature (CMT) of the thermosensitive block. This yields polymeric micelles with stealth coronas and hydrophobic cores that can accommodate hydrophobic drugs.[13] By fast heating ice-cold solutions of thermosensitive polymers above their CMT, they can form micelles with high drug loading and small size.[13] The preparation is accomplished in 1 min and avoids the use of large amounts of organic solvents.[17]

Unfortunately, in vivo pharmacokinetic studies of drug-loaded micelles showed rapid drug release in the circulation, probably due to a combination of extraction of the drug from the micelles and micellar destabilization.[18] It is hypothesized that, for example, albumin and lipoproteins in the circulation are able to bind amphiphilic polymer molecules, which can disrupt the dynamic equilibrium of micelles and unimers.[19−21] To tackle the instability of polymeric micelles, research has therefore been done on micelles' covalent cross-linking, including shell,[21,22] interface,[23] and core cross-linking.[18,24,25] Both in vitro and in vivo studies have demonstrated a substantially increased stability of cross-linked micelles leading

Received: February 13, 2013
Revised: April 2, 2013

   dx.doi.org/10.1021/bm400234c | *Biomacromolecules* XXXX, XXX, XXX−XXX

to the circulation kinetics of micelles comparable to that of pegylated liposomes.[18,26,27] However, paclitaxel (PTX)-loaded core-cross-linked micelles still showed fast drug release after i.v. administration in mice. This can likely be ascribed to the premature release and extraction of PTX from micellar core by plasma proteins. Therefore, the drug retention in the micelles should be improved to benefit from the good circulation time of cross-linked micelles.[28,29] To this end, doxorubicin has been covalently linked via a pH-sensitive hydrazone linker to the cross-linked core of mPEG-*b*-p(HPMAm-monolactate-*co*-HPMAm-dilactate) micelles.[30,31] A pharmacodynamic study showed a very promising therapeutic efficacy of these micelles in mice bearing B16F10 melanoma carcinoma.[32] In a recent study, dexamethasone has been coupled to the core of mPEG-*b*-p(HPMAm-monolactate-*co*-HPMAm-dilactate) micelles via a hydrolytically sensitive spacer and also showed excellent therapeutic effects in mice and rats models of rheumatoid arthritis.[33] However, chemical conjugation methods are not always feasible and might adversely affect the aimed therapeutic effect of conjugated drugs. Alternatively, physical interactions, including $\pi-\pi$ stacking,[34−41] hydrogen bonding,[42] stereocomplex formation,[43] and crystallinity[44] have been investigated to enhance the thermodynamic and kinetic stability of polymeric micelles but not yet in combination with thermosensitive, biodegradable polymers.

In the present study, aromatic groups modified *N*-(2-hydroxypropyl) methacrylamide (HPMAm), that is, *N*-(2-benzoyloxypropyl methacrylamide (HPMAm-Bz) and the corresponding naphthoyl analogue (HPMAm-Nt), that both can give $\pi-\pi$ stacking were copolymerized with HPMAm-lactate (HPMAm-Lac) to increase the stability, drug loading capacity, and drug retention of the obtained polymeric micelles. HPMAm-Bz and HPMAm-Nt were chosen due to the following attractive features. First, these monomers can easily be synthesized by modifying the hydroxyl group of HPMAm with benzoyl/naphthoyl chloride. Second, hydrolysis of the ester bond between the pendant groups and the hydrophobic block converts this block into hydrophilic p(HPMAm). The increased polarity of the corresponding block induces an increase of the CMT, dissociation of the micelles, and release of the payload at physiological temperature. Additionally, the hydrolyzed block, that is, p(HPMAm), has been clinically tested to be safe and p(HPMAm) with a molecular weight lower than 70 kDa will undergo renal excretion.[45] Two first-line anticancer drugs paclitaxel (PTX) and docetaxel (DTX) were chosen as model drugs (Figure 1) and encapsulated in the micelles.

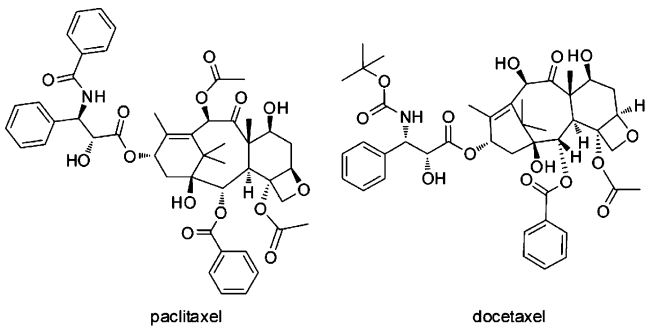

Figure 1. Chemical structures of paclitaxel (PTX, left) and docetaxel (DTX, right).

2. EXPERIMENTAL SECTION

2.1. Materials. *N*-(2-Hydroxypropyl) methacrylamide (HPMAm) was purchased from Zentiva, Czech Republic. The $mPEG_2$-ABCPA macroinitiator (M_n of mPEG = 5000 g·mol^{-1}), *N*-(2-hydroxypropyl) methacrylamide monolactate, and PEG-*b*-p(HPMAm-dilactate) were prepared as described previously.[46] Benzoyl chloride, 2-naphthoyl chloride, 8-anilino-1-naphthalenesulfonic acid hemimagnesium salt hydrate (8,1-ANS), pyrene, manganese(II) sulfate ($MgSO_4$), 4-methoxyphenol (4-MP), aluminum oxide (activated, basic), triethylamine (TEA), (2,2,6,6-tetramethylpiperidin-1-yl)oxyl (TEMPO), and *N*-(1,1-dimethyl-2-hydroxyethyl)-3-amino-2-hydroxy-propanesulfonic acid (AMPSO) were purchased from Sigma-Aldrich (Zwijndrecht, The Netherlands). Docetaxel (DTX) was purchased from Santa Cruz Biotechnology, Inc. (Heidelberg, Germany) and paclitaxel (PTX) was purchased from LC Laboratories (MA, U.S.A.). Acetonitrile (ACN), dichloromethane (DCM), diethyl ether, and *N*,*N*-dimethylformamide (DMF) were supplied by Biosolve Ltd. (Valkenswaard, The Netherlands).

2.2. Syntheses of *N*-(2-Benzoyloxypropyl) Methacrylamide and *N*-(2-Naphthoyloxypropyl) Methacrylamide (HPMAm-Bz/Nt). HPMAm-Bz/Nt were synthesized by reaction of the hydroxyl group of HPMAm with benzoyl chloride or 2-naphthoyl chloride, respectively, following a procedure described for modification of the terminal hydroxyl group of mPEG-*b*-oligocaprolactone oligomers by benzoylation or naphthoylation.[38] In detail, 10 g (0.070 mol) of HPMAm and 7.1 g (0.070 mol) of TEA were dissolved in 70 mL of dry DCM and 0.088 g (0.00070 mol) of 4-methoxyphenol (4-MP) was added as inhibitor. This solution was added dropwise to a solution of either benzoyl chloride (9.8 g, 0.060 mol) or 2-naphthoyl chloride (12.1 g, 0.060 mol) in 70 mL of dry DCM and the resulting solution was stirred for 24 h under a nitrogen atmosphere at room temperature. Subsequently, the formed and precipitated TEA·HCl was removed by filtration and the remaining solution was extracted three times with the same volume of reverse osmosis (RO) water to remove unreacted HPMAm and other water-soluble impurities. The DCM phase was dried with $MgSO_4$ and the inhibitor (4-MP) was removed by Al_2O_3 column chromatography. The column was washed with DCM, and the eluent was collected and evaporated under reduced pressure.

^{1}H NMR spectra were recorded using a Gemini 300 MHz spectrometer (Varian Associates Inc. NMR Instruments, Palo Alto, CA), using DMSO-d_6 as the solvent; the DMSO peak at 2.52 ppm was used as the reference line. Chemical shifts of both monomers (DMSO-d_6): 8.19 (t, CO-N<u>H</u>-CH_2), 5.60 and 5.30 (s, C<u>H_2</u>=C), 5.15 (q, CH_2−C<u>H</u>(CH_3)-O), 3.20 (t, NH-C<u>H_2</u>-CH), 1.80 (s, C<u>H_3</u>-C=C), 1.30 (d, H_2−CH(C<u>H_3</u>)-O). Chemical shifts of the benzoyl group (δ, ppm): 8.0 (d, 2H, aromatic CH), 7.61 (t, 1H, aromatic CH), 7.51 (t, 2H, aromatic CH). Chemical shifts of the naphthoyl group (δ, ppm): 8.21 (m, 1H, aromatic CH), 8.18 (d, 1H, aromatic CH), 8.05 (m, 3H, aromatic CH), 7.71 (m, 2H, aromatic CH).

2.3. Syntheses of ω-Methoxy Poly(ethylene glycol)-*b*-(*N*-(2-benzoyloxy/naphthoyloxypropyl) methacrylamide)-*co*-(*N*-(2-lactoyloxypropyl) methacrylamide) (mPEG-*b*-p(HPMAm-Bz/Nt-*co*-HPMAm-Lac)). The block copolymers were synthesized by free radical polymerization according to Soga et al.[47] using HPMAm-monolactate and HPMAm-Bz or HPMAm-Nt as the monomers and $mPEG_2$-ABCPA as the macroinitiator. The monomers were dissolved at a total concentration of 0.3 g/mL in dried ACN and the monomer-to-macroinitiator molar ratio was 150/1. To obtain block copolymers with different contents of HPMAm-Lac and HPMAm-Bz or HPMAm-Nt, the monomer ratios in the feed were varied between 100/0 to 25/75 (mol/mol), respectively. The solution was degassed by flushing with nitrogen for 15 min. Reactions were conducted at 70 °C for 18 h under a nitrogen atmosphere. The polymers were purified by precipitation in diethyl ether, and then dissolved in cold RO water and dialyzed against RO water at 4 °C for 24 h. The polymers were collected as white fluffy powders after freeze-drying.

The block copolymers are further denoted as mPEG-*b*-p(HPMAm-Bz_x-*co*-HPMAm-Lac_y) and mPEG-*b*-p(HPMAm-Nt_x-*co*-HPMAm-Lac_y), respectively, where x and y are the percentages of the

dx.doi.org/10.1021/bm400234c | *Biomacromolecules* XXXX, XXX, XXX−XXX

incorporated comonomers in the corresponding polymers determined by ^{1}H NMR spectroscopy.

2.4. Characterization of mPEG-*b*-p(HPMAm-Bz/Nt-*co*-HPMAm-Lac) Block Polymers. The ^{1}H NMR spectra were recorded as described in section 2.1. ^{1}H NMR of mPEG-*b*-p(HPMAm-Bz-*co*-HPMAm-Lac): 8.0 (b, 2H, aromatic CH), 7.55 (b, 1H, aromatic CH), 7.65 (b, 2H, aromatic CH), 7.35 (b, CO-NH-CH_2), 5.4 (d, $CH(CH_3)$-OH), 5.1 (b, NH-CH_2-CH(CH_3)-O-(Bz)), 4.8 (b, NH-CH_2-CH-(CH_3)-O-(Lac)), 4.1 (b, CH(CH_3)-OH), 3.40−3.60 (b, $mPEG_{5000}$ methylene protons, O-CH_2-CH_2), 3.2 (b, NH-CH_2-CH), 0.6−2.2 (b, the rest of the protons are from the methyl and backbone CH_2 protons).

^{1}H NMR of mPEG-*b*-p(HPMAm-Nt-*co*-HPMAm-Lac): 8.6 (b, 1H, aromatic CH), 8.05 (b, 3H, aromatic CH), 7.6 (b, 3H, aromatic CH), 7.35 (b, CO-NH-CH_2), 5.4 (b, $CH(CH_3)$-OH), 5.15 (b, NH-CH_2-CH(CH_3)-O-(Nt)), 4.8 (b, NH-CH_2-CH(CH_3)-O-(Lac)), 4.1 (s, CH(CH_3)-OH), 3.40−3.60 (b, $mPEG_{5000}$ methylene protons, O-CH_2-CH_2), 3.2 (b, NH-CH_2-CH), 0.6−2.2 (b, the rest of the protons are from the methyl and backbone CH_2 protons).

The number-average molecular weight (M_n) of the block copolymers was determined by ^{1}H NMR as follows: (a) the value of the integral of the mPEG protons divided by 448 (the average number of protons per one mPEG chain, M_n = 5000) gives the integral value for one mPEG chain, and (b) the number of HPMAm-Lac and HPMAm-Bz/Nt units in the polymers was determined from the ratio of the integral of the hydroxyl proton (5.4 ppm, 1H, CO-CH(CH_3)-OH) of HPMAm-Lac and aromatic protons of HPMAm-Bz (8.0 ppm, 2H, aromatic CH) or HPMAm-Nt (8.6 ppm, 1H, aromatic CH) to the integral of one mPEG chain. The M_n of the thermosensitive block was calculated from the resulting number of HPMAm-Lac and HPMAm-Bz/Nt units. The mol % of HPMAm-Bz/Nt in the thermosensitive block of the copolymer was determined by the following two equations:

$$\text{mol\% of HPMAm-Bz} = \frac{\text{integral } (H \text{ at } 8.0 \text{ ppm})/2}{\text{integral } (H \text{ at } 8.0 \text{ ppm})/2 + \text{integral } (H \text{ at } 4.1 \text{ ppm})}$$

$$\text{mol\% of HPMAm-Nt} = \frac{\text{integral } (H \text{ at } 8.6 \text{ ppm})}{\text{integral } (H \text{ at } 8.6 \text{ ppm}) + \text{integral } (H \text{ at } 4.1 \text{ ppm})}$$

GPC was conducted to measure the number average molecular weight (M_n), weight average molecular weight (M_w), and polydispersity (PDI, equal to M_w/M_n) using two serial Plgel 5 μm MIXED-D columns (Polymer Laboratories) and PEGs of narrow molecular weights as calibration standards. The eluent was DMF containing 10 mM LiCl, the elution rate was 0.7 mL/min, and the temperature was 40 °C.[47] GPC chromatograms of the macroinitiator and the synthesized polymer were deconvoluted to calculate the weight ratio of different fractions. The deconvolution was performed using IGOR Pro by the function of multipeak fitting.

2.5. Critical Micelle Temperature (CMT). The CMTs of the block copolymers were measured by dynamic light scattering (DLS). The polymers were dissolved for 16 h at 0 °C and at a concentration of 10 mg/mL in 120 mM ammonium acetate buffer (AAB) at pH 5.0. The solutions were heated in a water bath at 50 °C for 1 min with constant shaking to form micelles. Subsequently, the light scattering intensity (LSI) of the samples was continuously measured using DLS while the samples were cooled from 50 to 0.1 °C in 2 h. DLS was performed using a Malvern 4700 system (Malvern Ltd., Malvern, U.K.) consisting of an Autosizer 4700 spectrometer, a pump/filter unit, a model 2013 air-cooler argon ion laser (75 mW, 488 nm, equipped with a model 2500 remote interface controller, Uniphase), a water bath, and a computer with DLS software (PCS, version 3.15, Malvern). Autocorrelation functions were analyzed by the cumulants method (fitting a single exponential to the correlation function to obtain the mean size and the polydispersity) and the CONtIN routine (fitting a multiple exponential to the correlation function to obtain the distribution of particle sizes). The measurement angle was 90°. The light scattering intensity was plotted against the temperature and the onset on the *x*-axis, obtained by extrapolation of the LSI-temperatures curves to the baseline, was considered as the CMT.[48−51]

2.6. Critical Micelle Concentration (CMC). The CMCs of mPEG-*b*-p(HPMAm-Bz/Nt-*co*-HPMAm-Lac) were measured using two different fluorescent probes, namely, pyrene and 8-anilino-1-naphthalene-sulfonic acid magnesium salt (8,1-ANS), respectively. Because the naphthoyl group of the HPMAm-Nt containing polymers interfered with the excitation spectrum of pyrene (Supporting Information, Figure S2), pyrene was only used to measure the CMC of mPEG-*b*-p(HPMAm-Bz-*co*-HPMAm-Lac), whereas 8,1-ANS was used to measure the CMC of both types of polymers.

The block copolymers were dissolved in 4.5 mL of 120 mM ammonium acetate buffer (concentration ranging from 1×10^{-5} to 1 mg/mL) for 16 h at 0 °C. Next, 15 μL of pyrene dissolved in acetone (concentration of 1.8×10^{-4} M) was added and the solutions were subsequently incubated at 50 °C for 1 min. Next, the samples were cooled down to 37 °C (40 °C for mPEG-*b*-p(HPMAm-Bz_8-*co*-HPMAm-Lac_{92} because its CMT was around 37 °C) and incubated for 20 h to allow evaporation of acetone. Fluorescence excitation spectra of pyrene were obtained by a Horiba Fluorolog fluorometer (at an angle of 90°). The excitation spectra were recorded at 37 °C (40 °C for mPEG-*b*-p(HPMAm-Bz_8-*co*-HPMAm-Lac_{92}) from 300 to 360 nm with an emission wavelength at 390 nm. The excitation and emission band slits were 4 and 2 nm, respectively. The ratio of excitation intensity at 338 and 333 nm was plotted against polymer concentration to determine the CMC.[47]

The CMC was also determined using 8,1-ANS as a fluorescent probe. The block copolymers were dissolved at different concentrations as described above. A total of 200 μL of the micellar dispersion/polymer solution was pipetted into the wells of a black 96-well plate (Greiner). Next, to each well, 2 μL of 5 mM 8,1-ANS solution in DMF/water (1/10, v/v) was added and the solution/dispersion was then incubated at 37 °C (40 °C for mPEG-*b*-p(HPMAm-Bz_8-*co*-HPMAm-Lac_{92} because its CMT was around 37 °C) for 20 h. Fluorescence was measured using FluoSTAR (OPTIMA fluorimeter) at 37 °C. The excitation and emission wavelengths were 355 and 520 nm, respectively. The CMC was determined by plotting the fluorescence intensity against the polymer concentration.[38] The fluorescence of blank polymer solutions was measured as a reference.

2.7. Preparation of Empty and Drug-Loaded Micelles. Empty micelles were prepared by a fast heating method as described previously.[13] In short, the polymers were dissolved for 16 h at a concentration of 10 mg/mL in 120 mM AAB at pH 5.0 and 0 °C. Next, the polymer solutions were heated in a water bath at 50 °C for 1 min with constant shaking to form micelles. For paclitaxel (PTX) and docetaxel (DTX)-loaded micelles, 0.2 mL of the drug solution in ethanol (concentration ranging from 40 to 100 mg/mL) was added to 1.8 mL of an ice cold polymer solution and then immediately heated at 50 °C for 1 min. Subsequently, the micellar dispersions were incubated overnight at room temperature. The free drug was removed by filtration, a method frequently applied to remove nonentrapped drugs from micelles.[52−54] The size of the micelles was measured by DLS as described in section 2.5.

2.8. Drug Content Assay. The concentrations of the drugs loaded in the micelles were determined by UPLC analysis using Waters Acquity system consisting of a binary solvent manager, a sample manager and a UV detector. An Acquity HSS T3 1.8 μm column (2 × 50 mm) was used with a gradient eluent method at a flow rate of 1 mL/min, and a column temperature of 50 °C. Dispersions of drug-loaded micelles (0.1 mL) were diluted with 0.9 mL of ACN and subsequently vortexed to destabilize the micelles and dissolve the drug, and then centrifuged at 12.000 g for 10 min. A total of 7 μL of the supernatant was injected and the drug was measured at a wavelength of 227 nm. Samples of the drugs in ACN in a concentration range of 0.2 to 500 μg/mL were used for calibration. Encapsulation efficiency (EE) and loading capacity (LC) were calculated from the UPLC analysis results as follows:

Scheme 1. Synthesis of *N*-(2-Benzoyloxypropyl) Methacrylamide (HPMAm-Bz) and *N*-(2-Naphthoyloxypropyl) Methacrylamide (HPMAm-Nt)

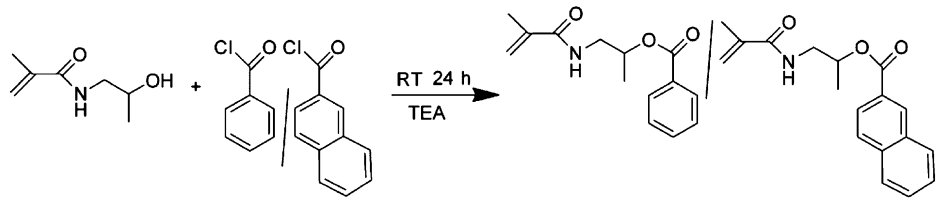

Scheme 2. Synthesis of mPEG-*b*-p(HPMAm-Bz/Nt-*co*-HPMAm-Lac)

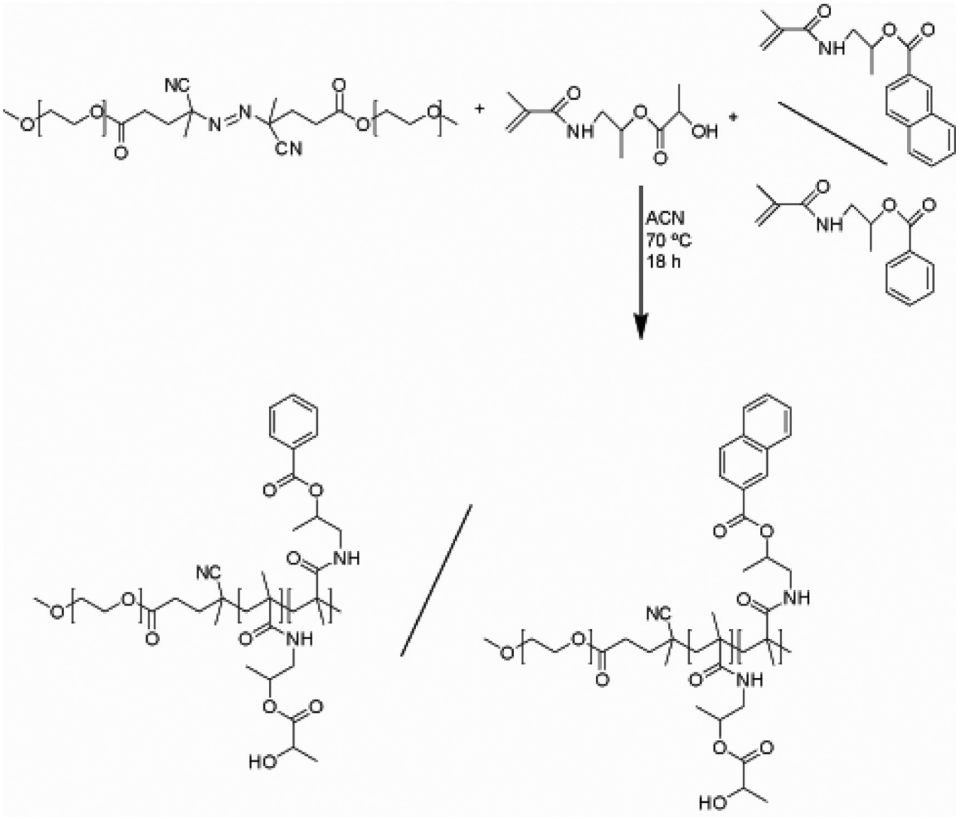

$$\mathrm{EE} = \frac{\text{concentration of drug measured}}{\text{concentration of drug added}} \times 100\%$$

$$\mathrm{LC} = \frac{\text{concentration of drug measured}}{\text{concentration of (drug measured + polymer added)}} \times 100\%$$

2.9. Transmission Electron Microscopy (TEM). TEM was performed using a Philips Tecnai12 equipped with a Biotwin lens and a LaB6 filament, operated at 120 kV acceleration voltage. In detail, micellar dispersions were diluted 10 times with 120 mM ammonium acetate buffer and droplets of the micellar dispersions (around 10 μL) were put on a piece of Parafilm. A glow discharged grid (copper 200 mesh grid with a carbon coated thin polymer film, Formvar or Pioloform on top) with the film side pointing down was placed on this droplet. After 3 min, the grid was taken off and the excess liquid was removed using a filter paper. Immediately, the grid with the film was put upside down on a 5 μL droplet of uranyl acetate 2%. After 1 min, the grid was taken off and the excess uranyl acetate was removed using filter paper. The grid was put on a filter paper and left for 5 min. Next, the grid was loaded into a TEM sample holder and Images were captured with a SIS Megaview II CCD-camera and processed with AnalySIS software.

2.10. In Vitro Stability and Drug Retention Study. The in vitro colloidal stability of drug-loaded and empty micelles based on mPEG-*b*-p(HPMAm-Nt$_{28}$-*co*-HPMAm-Lac$_{72}$) in pH 7.4 and 10.0 buffers at 37 °C was studied by monitoring the size and the light scattering intensity of the micelles by DLS. Empty micelles at a polymer concentration of 10 mg/mL were prepared in water as described in section 2.7. The pH of the micellar dispersion was adjusted to pH 10.0 or 7.4 by diluting 5-fold with 500 mM Na_2CO_3/$NaHCO_3$ pH 10.0 buffer or 500 mM NaH_2PO_4 pH 7.4 buffer. The samples were incubated at 37 °C and the DLS measurements were conducted continuously for 48 h.

Drug retention in the micelles in pH 7.4 phosphate buffer at 37 °C was evaluated by measuring the solubilized drug concentration in the micellar dispersion. PTX-loaded micelles were prepared as described in section 2.7 in pH 5.0 120 mM AAB and the pH was adjusted to 7.4 by diluting 5-fold with 500 mM phosphate pH 7.4 buffer. The released PTX crystallized and precipitated due to its low water solubility (0.3 μg/mL[38]). The samples were incubated at 37 °C with constant shaking, and aliquots were taken at different time points and centrifuged at 5000 g for 10 min to spin down the precipitated drug. Next, 0.1 mL of the supernatant was mixed with 0.3 mL of ACN and vortexed for 1 min, followed by centrifugation at 12.000 g for 10 min, and the drug concentration was determined by UPLC, as described in section 2.8.

dx.doi.org/10.1021/bm400234c | *Biomacromolecules* XXXX, XXX, XXX–XXX

2.11. In Vitro Cytotoxicity of Empty and PTX-Loaded Micelles. The in vitro cytotoxicity of empty and PTX-loaded mPEG-*b*-p(HPMAm-Bz$_{27}$-*co*-HPMAm-Lac$_{73}$) and mPEG-*b*-p(HPMAm-Nt$_{28}$-*co*-HPMAm-Lac$_{72}$) micelles was evaluated using B16F10 melanoma cells. mPEG-*b*-p(HPMAm-dilactate), which showed a good cytocompatibility, was used as a negative control, whereas Cremophor EL/ethanol (1/1, v/v; Taxol) was used as a positive control. B16F10 cells were maintained in Dulbecco's modified Eagle's medium (DMEM) supplemented with fetal bovine serum (FBS) (final concentration 10% v/v) and 1% of antibiotics. The cells were cultured at 37 °C and in a 5% CO_2 humidified atmosphere. Cells were seeded into 96-well plates at a density of (5×10^3 cells/well) and incubated for 24 h at 37 °C in a 5% CO_2 humidified atmosphere. Stock solutions of empty micelles (polymer = 9 mg/mL) and PTX-loaded micelles (PTX = 1 mg/mL, polymer = 9 mg/mL) were prepared in 5 mM HEPES buffer (pH 7.4), as described in section 2.7. PTX solubilized in Cremophor EL (Taxol) was prepared as follows: 12 mg of PTX was dissolved in 1.0 mL ethanol, and to this solution 1.0 mL Cremophor EL was added and the mixture was sonicated for 30 min.[10] The obtained Taxol formulation (PTX = 6 mg/mL) was diluted 6-fold with 5 mM HEPES buffer of pH 7.4. A formulation without PTX was prepared by mixing Cremophor EL and ethanol (1/1, v/v) followed by diluting with 5 mM HEPES buffer. The empty micelles and the Cremophor EL/ethanol solution were diluted with 5 mM HEPES pH 7.4 buffer to yield polymer concentrations ranging from 1 ng/mL to 1 mg/mL. The stock solutions of the drug formulations were diluted with 5 mM HEPES pH 7.4 buffer to yield PTX concentrations in the incubation medium ranging from 0.01 ng to 10 μg/mL. To evaluate the cytotoxicity, 100 μL of the different formulations and 100 μL of culture medium (DMEM + 10% FBS) were added to the cells. A total of 100 μL of 5 mM HEPES pH 7.4 buffer and 100 μL culture medium (DMEM + 10% FBS) were used as a control. The cells were incubated at 37 °C in a humidified atmosphere with 5% CO_2 and after 72 h the cell viability was determined using a XTT colorimetric assay.[55]

2.12. Detection of π−π Stacking in the Micelles by Solid State NMR Spectroscopy. Empty micelles of mPEG-*b*-p(HPMAm-Nt$_{18}$-*co*-HPMAm-Lac$_{82}$) were prepared in D_2O according to section 2.7. Solid-state NMR experiments were performed using a Bruker Avance III spectrometer equipped with a 4 mm double resonance (^{1}H, ^{13}C) probehead at 11.7 T static magnetic field. A MAS rate of 1 kHz and a ^{1}H radio frequency field strength of 66 kHz were used. 2D ^{1}H−^{1}H NOESY[56] experiments were conducted using a mixing time of 30 ms. Spectral referencing was done using adamantane.

3. RESULTS AND DISCUSSION

3.1. Syntheses of Monomers. *N*-(2-Benzoyloxypropyl) methacrylamide and *N*-(2-naphthoyloxypropyl) methacrylamide (HPMAm-Bz/Nt) were synthesized by the reaction of benzoyl chloride or 2-naphthoyl chloride with the hydroxyl group of HPMAm (Scheme 1). After purification, the products were obtained in a high yield (88% for HPMAm-Bz and 84% for HPMAm-Nt) as pale-yellow and yellow solid with a melting point of 53 and 89 °C, respectively. Their structures were confirmed by ^{1}H NMR spectroscopy.

3.2. Syntheses of Polymers. Block copolymers of mPEG-*b*-p(HPMAm-Bz/Nt-*co*-HPMAm-Lac) were synthesized via free radical polymerization using a previously published macroinitiator route (Scheme 2). mPEG with a number average molecular weight (M_n) of 5 kDa was the hydrophilic block, and the thermosensitive block was composed of HPMAm-Bz/Nt and HPMAm-Lac. The polymers were obtained in high yields after purification (72−90%). GPC analysis showed that the M_n of the synthesized polymers was between 14 and 22 kDa, which is close to that based on ^{1}H NMR analysis, and the PDIs (M_w/M_n) were around 1.7. GPC analysis (Figure S5) showed the presence of two small molecular weight shoulders (AUC lower than 10−15%) that had the same retention times as PEG 5 and 10 kDa (Figure S6), which indicates that small amounts of PEG 5 and 10 kDa homopolymers were present in the final polymer. The PEG 5 kDa likely originates from the macroinitiator synthesis, that is, PEG of 5 kDa that was not coupled to the azo initiator. The PEG 10 kDa is most likely formed due to the combination of two 5 kDa PEG free radicals during the polymerizations (Supporting Information, section 2). Furthermore, Figure S5 shows the presence of a double peak (at 17.7 and 18.5 min) apart from the PEG shoulders (at 20.0 and 21.4 min) in the GPC chromatogram of the synthesized polymer. Chain termination by recombination during free radical polymerization results in the formation of 10 kDa PEG chain and triblock copolymers of mPEG-p(HPMAm-Bz/Nt$_x$-*co*-HPMAm-Lac$_y$)-mPEG. The triblock copolymer due to its higher molecular weight has a lower retention time than the diblock mPEG-p(HPMAm-Bz/Nt$_x$-*co*-HPMAm-Lac$_y$), which could explain the bimodality of the main distribution of the GPC chromatogram. The weight ratio between these two populations, calculated by deconvoluting the GPC chromatogram, is around 1.5/1 (w/w; Figure S5). Chain termination during polymerizations can be suppressed by applying controlled radical polymerizations, including atom transfer radical polymerization (ATRP) and reversible addition−fragmentation chain transfer (RAFT) polymerization,[57,58] which is the subject of present investigations. Besides, the macroinitiator contained a small amount of ABCPA not coupled to two but to one methoxy PEG-OH chain (Supporting Information, Figure S6). This contamination yields, beside the diblock copolymer of mPEG-p(HPMAm-Bz/Nt$_x$-*co*-HPMAm-Lac$_y$), also a small fraction of homopolymer of p(HPMAm-Bz/Nt$_x$-*co*-HPMAm-Lac$_y$). This can be another reason for the multimodality of the GPC distribution. Overall, the mixtures of different polymers including di/triblock copolymers and homopolymers can form mixed micelles in aqueous solutions, which was demonstrated by DLS analysis of the micelles showing that there was only one size population with a low polydispersity (<1.1).

The ratios of HPMAm-Bz/Nt and HPMAm-Lac in the copolymers, determined by ^{1}H NMR spectroscopy, matched those of the feed (Supporting Information, Table S1). Four polymerization with 25 or 75% feed of HPMAm-Bz or HPMAm-Nt were quenched at an early stage and the composition of the formed polymers was examined by ^{1}H NMR spectroscopy. The results showed that copolymer compositions were close to that of feed (Supporting Information, Table S2), which points out that HPMAm-Bz/Nt and HPMAm-Lac have similar relativities, which ensures that random copolymers of the different monomers were formed.

3.3. Critical Micelle Temperature (CMT). Figure 2 shows the CMTs of the mPEG-*b*-p(HPMAm-Bz/Nt-*co*-HPMAm-Lac) with different HPMAm-Bz/Nt content, measured by DLS as the disappearance of light scattering upon cooling. This figure shows that the CMT of mPEG$_{5000}$-p(HPMAm-Lac) was 55 °C. The CMT decreased with increasing HPMAm-Bz/Nt content in the block copolymers which can be explained by hydrophobic interaction and π−π stacking between the aromatic groups of the thermosensitive block. The lowest CMTs (2.5 and 0.7 °C) of mPEG-*b*-p(HPMAm-Bz/Nt-co-HPMAm-Lac) were obtained for polymers containing 26.9 mol % HPMAm-Bz and 28.4 mol % HPMAm-Nt, respectively. In other words, the polymers with the HPMAm-Bz/Nt content between 11.8% and

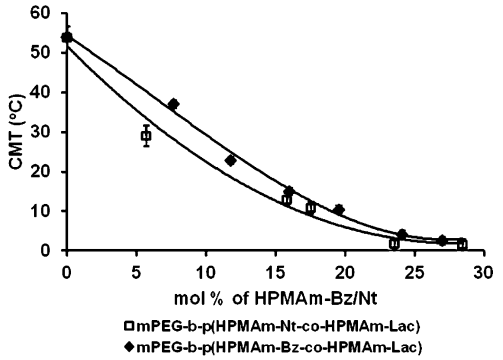

Figure 2. CMTs of mPEG-*b*-p(HPMAm-Bz/Nt-*co*-HPMAm-Lac) as a function of mol % of HPMAm-Bz/Nt (n = 3).

approximately 28.4% have CMTs between 25 and 0 °C, and are therefore of interest for pharmaceutical application. Higher contents of aromatic monomers gave polymers that were insoluble in water at 0 °C.

3.4. Critical Micelle Concentration (CMC). Figure 3 shows that the CMC of mPEG-*b*-p(HPMAm-Bz-*co*-HPMAm-

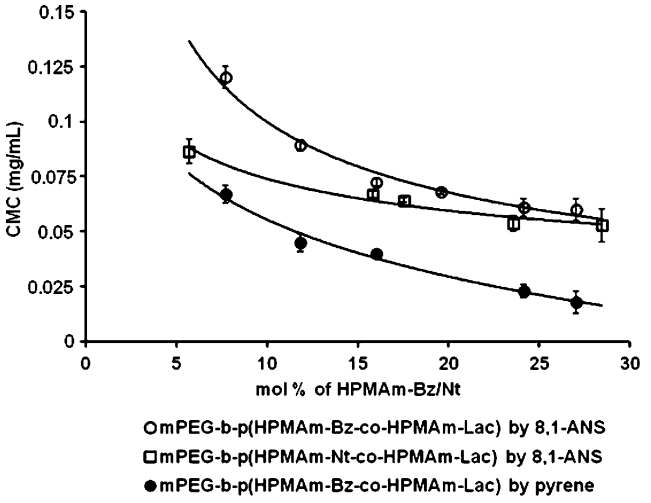

Figure 3. CMC as a function of mol % of HPMAm-Bz/Nt in the copolymers at 37 °C (n = 3).

Lac) using pyrene as a fluorescence probe decreased from 0.067 to 0.018 mg/mL with increasing content of HPMAm-Bz from 8 to 27%. The CMC of mPEG-*b*-p(HPMAm-Bz_{24}-*co*-HPMAm-Lac_{76}) was lower than that of mPEG-*b*-p(HPMAm-dilactate) (0.023 and 0.080 mg/mL, respectively), while they have similar CMTs of around 4 °C,[46] and therefore it is suggested, $\pi-\pi$ stacking and hydrophobicity of the aromatic groups contribute to the lower CMC.

When 8,1-ANS was used as fluorescent probe, the CMCs were approximately two times higher for mPEG-*b*-p(HPMAm-Bz-*co*-HPMAm-Lac) than those obtained using pyrene (Figure 3), likely because the interactions between the hydrophobic block of the polymers and the more hydrophilic 8,1-ANS is weaker than that of the very hydrophobic pyrene.[37] Corresponding CMC values decreased from 0.12 to 0.060 mg/mL with increasing HPMAm-Bz content (from 7.7 to 26.9%), while those of mPEG-*b*-p(HPMAm-Nt-*co*-HPMAm-Lac) were slightly lower and decreased from 0.087 to 0.054 mg/mL with increasing HPMAm-Nt content from 5.7 to 28.4%. This suggests a slightly stronger interaction between the polymer chains in micelles of the latter copolymers.

3.5. Preparation and Characterization of Empty and Drug-Loaded Micelles. The *Z*-average hydrodynamic diameters of empty micelles, prepared by the fast heating method[13] and determined by DLS ranged from 30 to 50 nm, with very low polydispersities (<0.1, Figure 4). The lower sizes of those

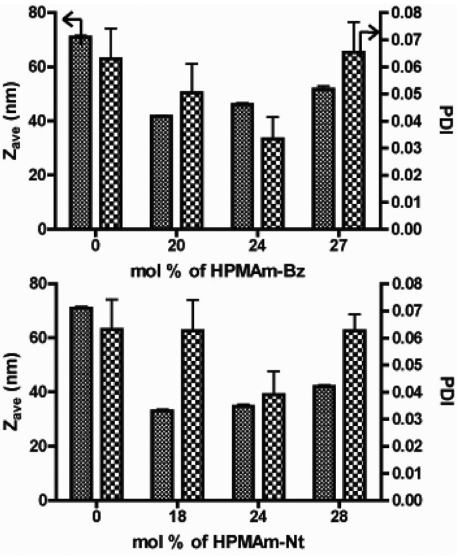

Figure 4. *Z*-average hydrodynamic diameter (Z_{ave}, filled bars) and polydispersity index (PDI, blocky bars) of empty polymeric micelles. A total of 0% corresponds to mPEG-*b*-p(HPMAm-dilactate), and others are mPEG-*b*-p(HPMAm-Bz/Nt-*co*-HPMAm- Lac), with the corresponding amounts of HPMAm-Bz/Nt in the polymers measured by ^{1}H NMR spectroscopy, respectively. All measurements were performed at 25 °C (n = 3).

micelles as compared to micelles prepared from $mPEG_{5000}$-*b*-p(HPMAm-dilactate) (70 nm, Figure 4) is due to $\pi-\pi$ stacking and the high hydrophobicity of the aromatic groups leading to a more condensed core of mPEG-*b*-p(HPMAm-Bz/Nt-*co*-HPMAm-Lac) micelles.

Dispersions of DTX-loaded micelles of mPEG-*b*-p(HPMAm-Bz_{25}-*co*-HPMAm-Lac_{75}) and mPEG-*b*-p(HPMAm-Nt_{14}-*co*-HPMAm-Lac_{86} prepared at a polymer/drug weight ratio of 1.8/1 were opalescent and homogeneous, while those of mPEG-*b*-p(HPMAm-dilactate) were cloudy (Figure 5). After subsequent removing precipitated/aggregated DTX by filtration through a 0.45 μm membrane, the encapsulation efficiencies (EE) of DTX in the micellar dispersions were 53.9 ± 1.3, 64.7 ± 2.1, and 2.9 ± 0.2%, for mPEG-*b*-p(HPMAm-Bz_{24}-*co*-HPMAm-Lac_{76}), mPEG-*b*-p(HPMAm-Nt_{15}-*co*-HPMAm- Lac_{85}, and mPEG-*b*-p(HPMAm-dilactate) micelles, respectively. This indicates that the micelles containing the aromatic groups are better capable to solubilize/disperse DTX. TEM images of drug-loaded and empty micelles are shown in Figure 6.

The drug loading capacity of the micelles was evaluated for the chemotherapeutic drugs PTX and DTX[45] that both have aromatic groups and are characterized by a high hydrophobicity (log *P*s are 4.7 and 4.1, respectively[37]). Figure 7 shows that at a feed drug concentration of 4 mg/mL mPEG-*b*-p(HPMAm-dilactate) had a loading capacity (LC) of 17.8 ± 0.4 and 8.2 ± 0.6% for PTX and DTX, respectively. This was associated with a rather low EE of 48.7 ± 2.1 and 20.1 ± 1.2%, respectively.

dx.doi.org/10.1021/bm400234c | *Biomacromolecules* XXXX, XXX, XXX−XXX

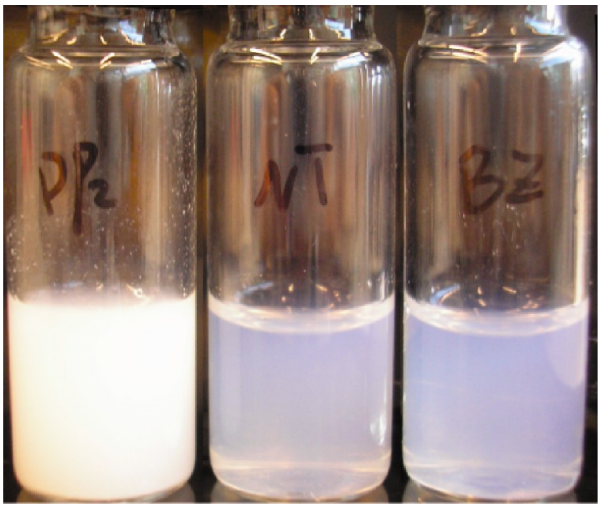

Figure 5. Photograph of DTX-loaded micelles dispersions. Feed concentrations were 5 mg/mL DTX and 9 mg/mL of the different polymers. From left to right: mPEG-*b*-p(HPMAm-dilactate), mPEG-*b*-p(HPMAm-Nt_{18}-*co*-HPMAm-Lac_{82}) and mPEG-*b*- p(HPMAm-Bz_{24}-*co*-HPMAm-Lac_{76}).

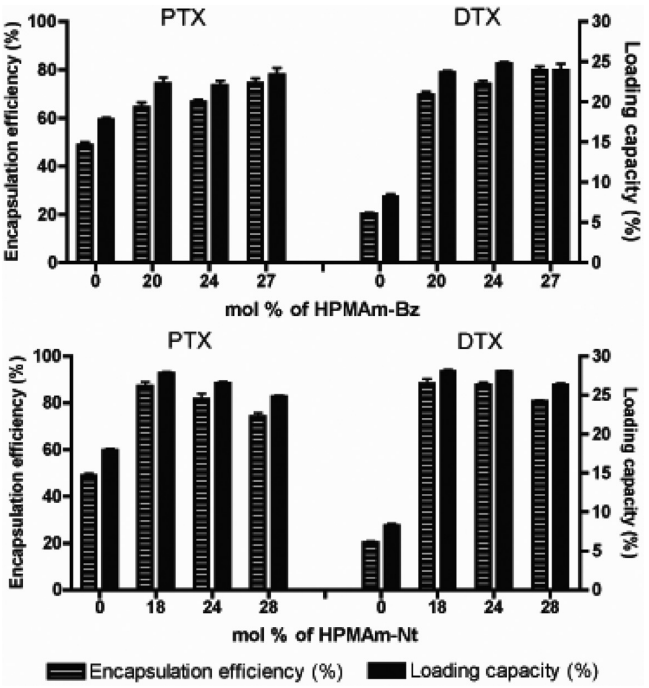

Figure 7. Encapsulation efficiency (EE) and loading capacity (LC) of PTX- and DTX-loaded micelles (feed drug and polymer concentrations were 4 and 9 mg/mL); 0% corresponds to mPEG-*b*-p(HPMAm- dilactate); the other polymers are mPEG-*b*-p(HPMAm-Bz/Nt-*co*-HPMAm-Lac) with different amounts of HPMAm-Bz/Nt, respectively (n = 3).

This polymer had a higher loading capacity for PTX than DTX, which can probably be ascribed to a better compatibility of PTX and the polymer than that with DTX. Interestingly, mPEG-*b*-p(HPMAm-Bz/Nt-*co*-HPMAm-Lac) showed a significantly increased LC compared to mPEG-*b*-p(HPMAm-dilactate). When the feed concentrations of drug and polymers were 4 and 9 mg/mL, the highest LCs were 27.8 ± 0.3 and 28.0 ± 0.4% for PTX and DTX, and the EEs were 87.1 ± 3.2 and 88.2 ± 3.6%, respectively.

Figure 7 shows that when feed concentrations of drug and polymers were 4 and 9 mg/mL, respectively, mPEG-*b*-p(HPMAm-Bz_{24}/Nt_{18}-*co*-HPMAm-$Lac_{76/82}$) were the polymers that displayed the highest EE and LC for PTX and DTX. Therefore, the influence of increasing feed drug concentration on the EE and LC at a fixed concentration of these polymers was evaluated, with mPEG-*b*-p(HPMAm-dilactate) as control (Table 1, Figures S8 and S9). In Figure S8, it is clear that the EE of DTX decreased when feed concentration increased from 4 to 10 mg/mL. On the other hand, the LC of DTX peaked at feed concentration of 7 mg/mL (Figure S9). Afterward, passing the upper limit of the loading capacity results in precipitation of the drug, and therefore low EE.[59−61] The highest LCs obtained for the DTX were 29.5 ± 0.5 and 33.5 ± 0.9 for mPEG-*b*-p(HPMAm-Bz_{24}-*co*-HPMAm-Lac_{76}) and mPEG-*b*-p(HPMAm-Nt_{18}-*co*-HPMAm-Lac_{82}), respectively (Table 1). To the best of our knowledge, polymeric micelles with the highest PTX loading reported in literature are those based on PEG-*b*-p(2-(4-vinylbenzyloxy)-*N*,*N*-diethylnicotinamide).[38] For those micelles, the LC of 37.4% for PTX was calculated by weight of drug per weight of polymer. For comparison, when our results are calculated in that way, the LC of the mPEG-*b*-p(HPMAm-Nt_{18}-*co*-HPMAm-Lac_{82}) would be equal to 50.4% for DTX. In other words, we can state that the loading capacity of our micelles is unprecedentedly high.

Figure 7 shows that with 4 mg/mL of feed drug concentration, the LC did not increase with increasing HPMAm-Bz/Nt content, which can be ascribed to an enhanced interaction between the hydrophobic blocks of the polymers with increasing HPMAm-Bz/Nt content, which would reduce

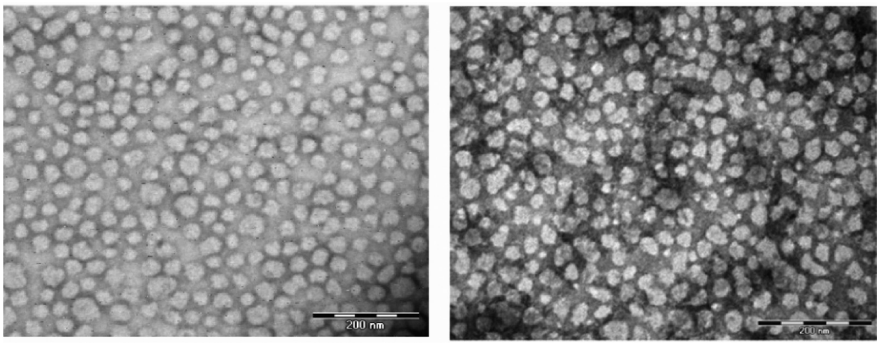

Figure 6. TEM images of empty and DTX-loaded polymeric micelles: polymer, mPEG-*b*-p(HPMAm-Bz_{27}-*co*-HPMAm-Lac_{73}); left, empty micelles; right, DTX-loaded micelles. Feed concentrations of the drug and polymer were 4 and 9 mg/mL, respectively.

dx.doi.org/10.1021/bm400234c | *Biomacromolecules* XXXX, XXX, XXX−XXX

Table 1. DTX Loading and Molar Ratios of DTX/Polymer/Aromatic Groups of Various Micelles for Different Feed Ratios of Polymer and Drug

aromatic comonomer content[a]	feed drug concentration (mg/mL)	EE (%)	LC (%)	DTX/polymer[b]	DTX/aromatic groups[b]
24% HPMAm-Bz	10	10.1 ± 0.4	10.1 ± 0.2	3.7	0.4
18% HPMAm-Nt	10	33.1 ± 1.1	26.9 ± 0.7	15.5	2.2
0%	10	2.4 ± 0.1	2.6 ± 0.3	1.2	NA
24% HPMAm-Bz	7	53.9 ± 1.3	29.5 ± 0.5	14.0	1.4
18% HPMAm-Nt	7	64.7 ± 2.1	33.3 ± 0.9	21.2	3.0
0%	7	2.9 ± 0.2	2.1 ± 0.3	1.0	NA
24% HPMAm-Bz	5	67.8 ± 1.9	27.4 ± 0.6	12.6	1.8
18% HPMAm-Nt	5	70.7 ± 2.6	28.2 ± 0.3	16.5	2.3
0%	5	21.1 ± 1.3	10.5 ± 0.2	5.2	NA
24% HPMAm-Bz	4	74.2 ± 2.3	24.8 ± 0.3	11.0	1.4
18% HPMAm-Nt	4	88.1 ± 3.6	28.1 ± 0.4	16.5	2.3
0%	4	20.1 ± 1.2	8.2 ± 0.3	4.0	NA

[a]0% corresponds to mPEG-*b*-p(HPMAm-dilactate); the other polymers are mPEG-*b*-p(HPMAm-Bz/Nt-*co*-HPMAm-Lac) with different amounts of HPMAm-Bz/Nt, respectively (n = 3). [b]mol/mol.

the space for encapsulation of drug molecules. A similar effect that an increasing hydrophobicity of polymers decreased their LC was reported for micelles based on cholesterol-modified polymers.[62]

The ratios of DTX to the number of aromatic groups in the micelles and that of DTX to the polymers (mol/mol) were calculated (Table 1). For the polymers with aromatic groups, the ratio of DTX to polymer with a drug feed concentration of 7 mg/mL and a polymer concentration of 9 mg/mL was up to 20 times higher as compared to mPEG-*b*-p(HPMAm-dilactate). The HPMAm-Nt containing polymer encapsulated around two times more DTX molecules than the HPMAm-Bz polymer. The ratio of drug/aromatic groups also showed that more DTX molecules were associated with the HPMAm-Nt than HPMAm-Bz groups, likely due to the more hydrophobic character of HPMAm-Nt and its better $\pi-\pi$ stacking with the drug. The difference of DTX molecules associated with HPMAm-Bz and HPMAm-Nt groups was most pronounced when the drug feed concentration was increased from 5 to 10 mg/mL.

Figure 8 shows that the size of drug-loaded micelles at feed concentrations of drug and polymer of 4 and 9 mg/mL, respectively, increased compared with that of empty micelles (30−50 nm, Figure 4). Both PTX- and DTX-loaded mPEG-*b*-p(HPMAm-dilactate) micelles had a size of around 110 nm, however, the size of drug-loaded mPEG-*b*-p(HPMAm-Bz/Nt-*co*-HPMAm-Lac) size was between 60 and 80 nm (polydispersity between 0.04 and 0.23), despite their larger drug contents. The smaller size of the micelles carrying aromatic comonomers indicates that their cores are more condensed, which is due to the $\pi-\pi$ stacking and hydrophobic effect of the aromatic groups.

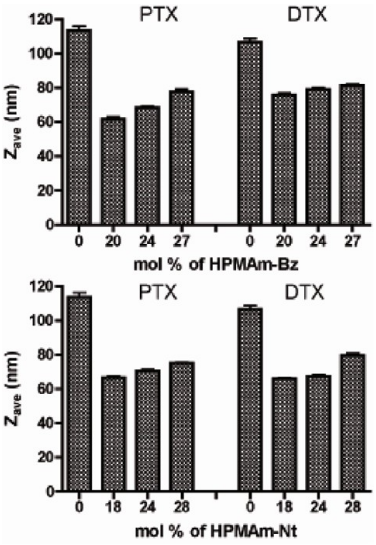

Figure 8. Z-average hydrodynamic diameter (Z_{ave}) of drug-loaded polymeric micelles at 25 °C. A total of 0% corresponds to mPEG-*b*-p(HPMAm-dilactate); the others polymers are mPEG-*b*-p(HPMAm-Bz/Nt-*co*-HPMAm-Lac) with different amounts of HPMAm-Bz/Nt (n = 3).

3.6. In Vitro Stability and Drug Retention Studies. The size and light scattering intensity (LSI) of empty and drug-loaded micelles of mPEG-*b*-p(HPMAm-Nt_{24}-*co*-HPMAm-Lac_{76}) in pH 7.4 buffer were stable for at least 48 h at 37 °C (Figures 9 and 10), which indicates a good colloidal stability. It has been proven that the hydrolysis of the side groups in the pH range 7 to 10 is first order in OH^- concentration,[63] which allows calculation of the stability under physiological conditions using accelerated degradation conditions. Therefore, a hydrolytic stability study was also conducted at pH 10.0. When the micelles were incubated in pH 10.0 buffer, they began to swell after 2 h, accompanied by a strong increase of the LSI, and dissociated after 7 h as reflected by the sudden decrease in the LSI. This behavior is similar to what has been reported for PEG-*b*-p(HPMAm-dilactate) based micelles[47] and is caused by the hydrolysis of the lactate and naphthoate side groups of HPMAm, followed by hydration of the core of the micelles due to its increased hydrophilicity. Destabilization of the micelles occurs when the lower critical solution temperature (LCST) of the polymer increases such that it passes the incubation temperature of 37 °C.[47] The $t_{1/2}$ of the hydrolysis of HPMAm-Lac at 37 °C and pH 10.0 is calculated to be 0.28 h based on a previous study,[63] and the hydrolysis study of HPMAm-Nt (Supporting Information, section 4) showed that the $t_{1/2}$ was 6.8 h under the same condition. Therefore, at the early stage of the micelles' destabilization, the hydrolysis of HPMAm-Lac contributed mainly to the hydration of the micelles' core, whereas the full dissociation of the micelles is probably related to the hydrolysis of the aromatic units. According to the degradation study of the monomers HPMAm-Bz/Nt (Supporting Information, section 4) and HPMAm-Lac,[63] the hydrolysis

dx.doi.org/10.1021/bm400234c | *Biomacromolecules* XXXX, XXX, XXX−XXX

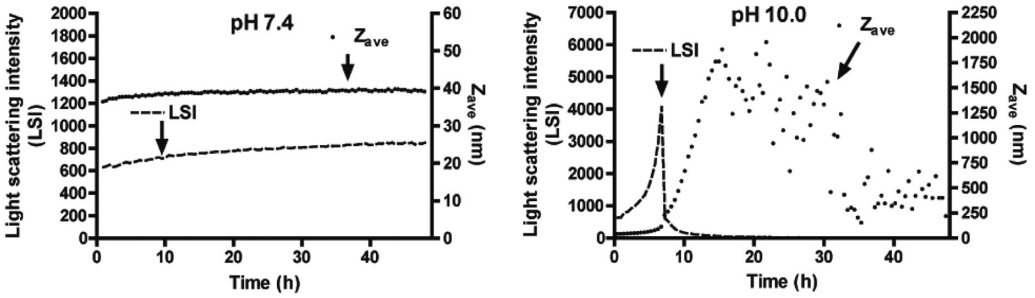

Figure 9. Stability of empty micelles of mPEG-*b*-p(HPMAm-Nt$_{25}$-*co*-HPMAm-Lac$_{75}$) at pH 7.4 (left) and 10.0 (right) measured by DLS at 37 °C.

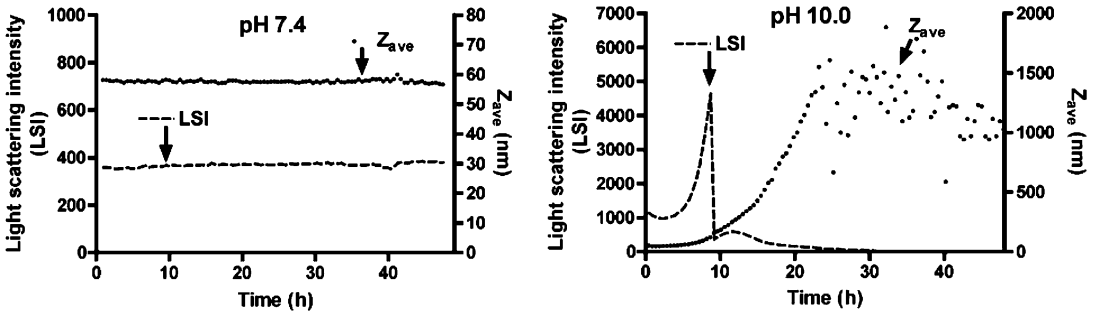

Figure 10. Stability of PTX-loaded micelles of mPEG-*b*-p(HPMAm-Nt$_{24}$-*co*-HPMAm-Lac$_{76}$) at pH 7.4 (left) and 10.0 (right) measured by DLS at 37 °C.

is a first-order reaction in hydroxyl ion concentration. The degradation rate of the monomers at pH 10.0 is therefore about 400 times faster than that at pH 7.4. Consequently, based on the swelling and dissociation time of the micelles at pH 10.0, it is calculated that the micelles start to swell after ~800 h and fully dissociate after ~3000 h of incubation at pH 7.4.

The micellar dispersion turned clear after hydrolysis at 37 °C and pH 10.0. This means that after hydrolysis, the polymers are fully water-soluble and can be eliminated by renal filtration[44] as the molecular weights are below 31 kDa (Supporting Information, Table S1). Additionally, the ester bond between mPEG$_{5000}$ and the thermosensitive block is hydrolyzable ($t_{1/2}$ = 34 h at pH 8.5 and 37 °C),[63] and the molecular weight of the polymers therefore further decreases after hydrolysis of the ester bond connecting the two blocks.

A release study was carried out under nonsink conditions. The water solubility of PTX is rather low (0.3 μg/mL), and it is consequently practically difficult to maintain sink conditions during release. To explain, to keep the PTX concentration in the medium below the saturation concentration requires a large volume or a frequent refresh of the release medium, or addition of surfactants to solubilize the released PTX. However, the first two options might result in a too low drug concentration for detection and in destabilization of the micelles due to passing the CMC of the polymers. The addition of surfactants also might result in destabilization of the micelle and/or the formation of mixed micelles. Nevertheless, despite the nonsink conditions, the payload of mPEG-*b*-p(HPMAm-dilactate) micelles was almost fully released and precipitated after 240 h of incubation at pH 7.4. On the contrary, there was still around 50% of loaded PTX solubilized in micelles of mPEG-*b*-p(HPMAm-Bz/Nt-*co*-HPMAm-Lac) at the same time (Figure 11). Therefore, a better retention of PTX in the micelles with the aromatic groups (benzoyl and naphthoyl) is shown as compared to micelles lacking aromatic units in their polymer chains, which can be explained by $\pi-\pi$ stacking and

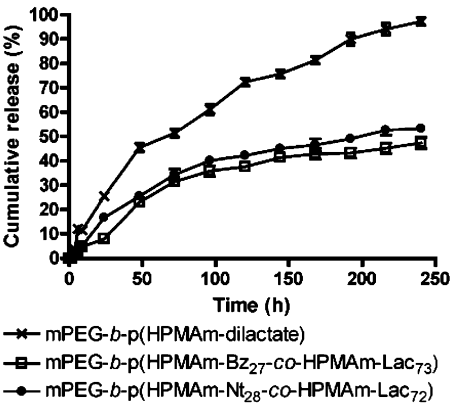

Figure 11. PTX release from micelles in PBS 7.4 at 37 °C (n = 3).

hydrophobic interaction between aromatic groups, the micelles' core, and those of the drug.

3.7. In Vitro Cytotoxicity Study. The in vitro cytotoxicity of both PTX-loaded and empty micelles based on mPEG-*b*-p(HPMAm-Bz/Nt-*co*-HPMAm-Lac) was studied using B16F10 cells. For comparison, mPEG-*b*-p(HPMAm-dilactate) micelles, which have a good cytocompatibility and Cremophor EL/ethanol with and without PTX, were included as well (Figure 12). Cremophor/ethanol showed a strong cytotoxicity at high concentrations (0.1 and 1.0 mg/mL), while the polymeric micelles hardly affected the cells' viability up to 1 mg/mL. At high concentrations (>0.01 mg/mL), micelles of mPEG-*b*-p(HPMAm-Bz/Nt-*co*-HPMAm-Lac) showed a slightly higher cytotoxicity than the mPEG-*b*-p(HPMAm-dilactate) ones. Figure 12 also shows that the cytotoxicity of mPEG-*b*-p(HPMAm-Nt$_{28}$-*co*-HPMAm-Lac$_{72}$) micelles was slightly higher than that of mPEG-*b*-p(HPMAm-Bz$_{27}$-*co*-HPMAm-Lac$_{73}$) micelles. Figure 13 shows that PTX-loaded polymeric micelles at low PTX concentration (up to 0.1 μg/mL) showed

dx.doi.org/10.1021/bm400234c | *Biomacromolecules* XXXX, XXX, XXX−XXX

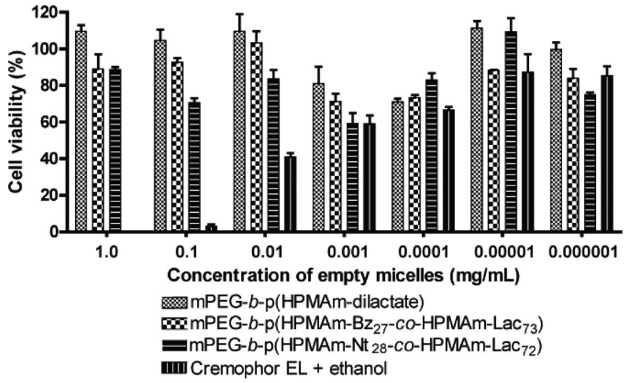

Figure 12. In vitro cytotoxicity of empty micelles on B16F10 after 72 h of incubation (n = 3).

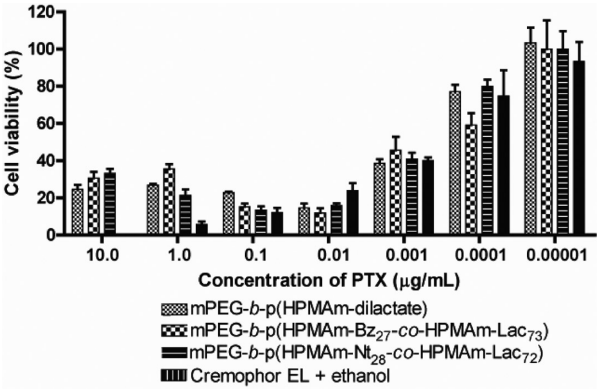

Figure 13. In vitro cytotoxicity of PTX formulations on B16F10 after 72 h of incubation (n = 3).

comparable cytotoxicity on B16F10 as Taxol. At both 1 and 10 μg/mL of PTX, Taxol showed a higher cytotoxicity than PTX-loaded polymeric micelles formulations which can be ascribed to the high toxicity of the Cremophor EL/ethanol vehicle. The concentrations of the polymers were below the CMC at PTX concentration <2 μg/mL and thus the drug was present in its free form in the cell culture medium. At the PTX concentration of 10 μg/mL, the polymer concentration was higher than the CMC. However, as seen in Figure 11, around 30% of PTX was released in 72 h (the incubation time of the cell with the formulations). This means that the cytotoxicity of the formulation is therefore likely due to released PTX either in the incubation medium and/or after endocytosis of the micelles in the cytosol. The released PTX concentration in the medium for the micellar formulation of 10 μg/mL of PTX is probably at least 3 μg/mL, which explains that the cell viability of 10 μg/mL of PTX was similar to that of 1 μg/mL of PTX.

3.8. Detection of the $\pi-\pi$ Stacking in Micelles. We conducted one- and two-dimensional ^{1}H solid-state NMR experiments on the micellar suspension prepared in D_2O with a polymer concentration of 10 mg/mL at 37 and 1 °C. Magic Angle Spinning (MAS,[64]) was employed to increase spectral resolution.

In general, such solid-state NMR experiments report on molecular structure via the measurement of isotropic chemical shifts and internuclear interactions, that is, dipolar spin−spin interactions. The chemical shift of hydrogen atoms is strongly influenced by external electrons providing a means to study packing of π-electron systems. In particular, $\pi-\pi$ interactions lead to a shift of aromatic ^{1}H NMR signals to lower ppm values.[65,66] In addition, cross peak intensities observed in two-dimensional correlation experiments such as NOESY[67] spectra report on internuclear geometry.[65,68,69] Intermolecular interactions such as $\pi-\pi$ stacking should, hence, increase the magnitude and number of cross peak correlations among aromatic protons. Finally, previous solid-state NMR work in semisolid systems such as hydrogels[70,71] has shown that a decrease in molecular tumbling leads to an increase in solid-state NMR line width. Figure 14 compares two 1D ^{1}H spectra

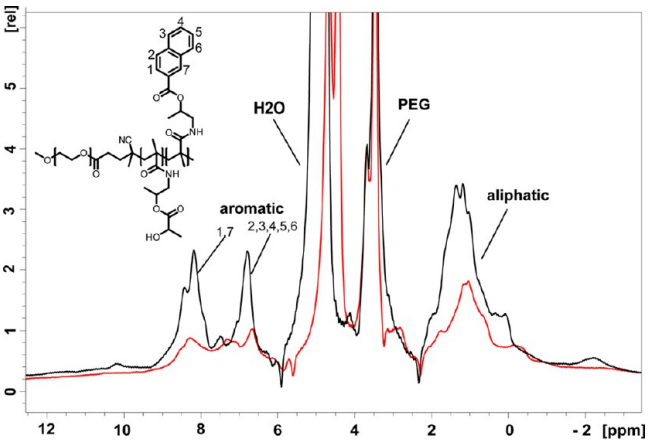

Figure 14. Comparison of 1D solid-state NMR ^{1}H spectra obtained under MAS at 37 °C (red) and 1 °C (black). Numbering of the aromatic proton positions is given in the inset.

obtained at 37 °C (red) and 1 °C (black) using an MAS rate of 1 kHz. Upon increasing the temperature, aromatic signals broadened significantly in line with an overall increase in effective molecular size.[70,71] Furthermore, aromatic signals shifted toward lower ppm values, as expected for $\pi-\pi$ interactions. To investigate such interactions by 2D NMR, we acquired 2D NOESY[67] spectra obtained at both temperatures (Figure 15). In general, cross peaks were more intense at 37 °C (red) and correlations shifted upfield. Although a detailed structural analysis is precluded because cross-peak intensities not only depend on distance but also molecular correlation time and MAS rate[69] the most likely explanation for the observed correlations (indicated by dashed boxes) are proximal intra- or intermolecular nuclear interactions within aromatic rings.[71] Taken together, the NMR results (line width, chemical shifts and 2D cross peak intensities) are consistent with an overall reduction in molecular mobility due to micelle formation that involves $\pi-\pi$ stacking[66,65] among aromatic moieties at higher temperature.

CONCLUSION

Thermosensitive amphiphilic polymers of mPEG-*b*-p(HPMAm-Bz/Nt-*co*-HPMAm-Lac) were synthesized and they self-assembled into polymeric micelles above their critical micelle temperature and critical micelle concentration. Solid-state NMR data are consistent with the formation of $\pi-\pi$ stacking in the micellar core among the aromatic groups. The poorly water-soluble anticancer drugs paclitaxel and docetaxel were encapsulated into the polymeric micelles with an unprecedented high loading efficiency. The mPEG-*b*-p(HPMAm-Bz/Nt-*co*-HPMAm-Lac) micelles had a better drug loading and retention compared with mPEG-*b*-p(HPMAm-

dx.doi.org/10.1021/bm400234c | Biomacromolecules XXXX, XXX, XXX−XXX

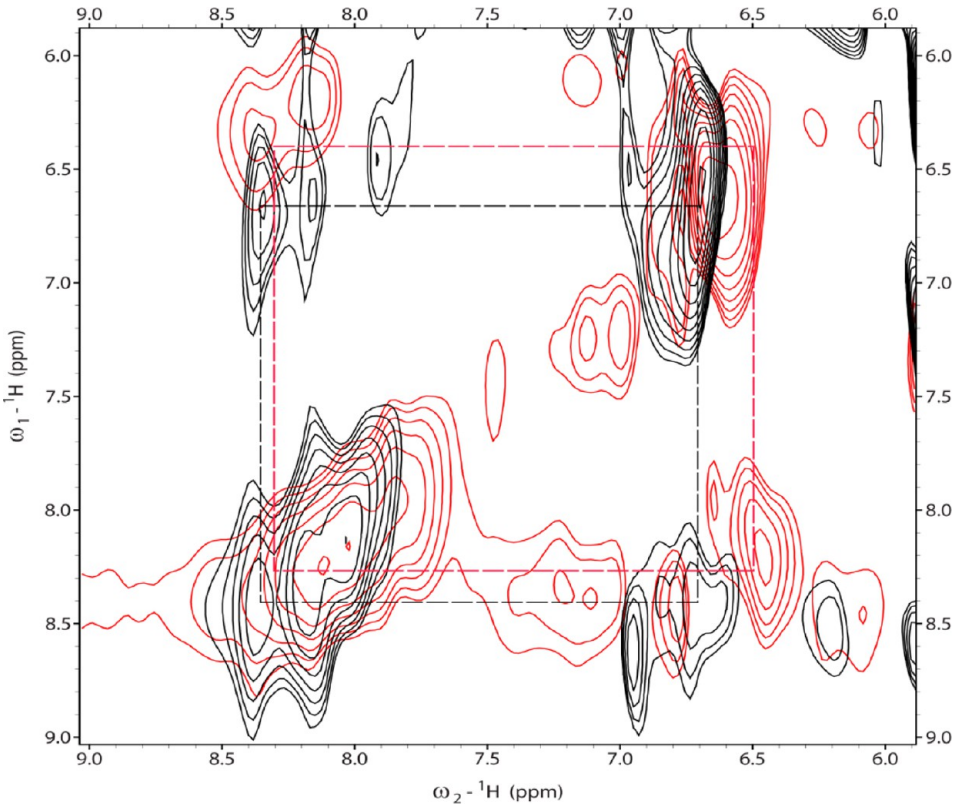

Figure 15. Spectral cutouts of 2D ^{1}H−^{1}H NOESY spectra obtained at 37 °C (red) and 1 °C (black) using a mixing time of 30 ms. Dotted lines connect diagonal and cross-peak correlations.

dilactate) micelles that do not contain aromatic units in the polymer chains due to $\pi-\pi$ stacking and hydrophobic interaction by aromatic groups. The empty polymeric micelles did not affect the viability of B16F10 cells up to 1 mg/mL and PTX-loaded polymeric micelles showed comparable cytotoxicity on B16F10 as Taxol, which means that the therapeutic effect of PTX was not affected by loading it into the polymeric micelles. The high loading capacity, strong drug retention in the micelles and low cytotoxicity of the synthetic polymers show the potential for in vivo application. The paclitaxel-loaded micelles will be further evaluated in vivo in a suitable animal model.

■ ASSOCIATED CONTENT

Ⓢ Supporting Information

The detailed GPC and ^{1}H NMR characterizations of polymers, excitation spectra of the polymers and pyrene, and HPMAm-Bz/Nt hydrolytic degradation are described. This material is available free of charge via the Internet at http://pubs.acs.org.

■ AUTHOR INFORMATION

Corresponding Author

*Tel.: + 31 30 253 6964. Fax: + 31 30 251 7839. E-mail: w.e.hennink@uu.nl.

Notes

The authors declare no competing financial interest.

■ ACKNOWLEDGMENTS

The research was partially supported by China Scholarship Council. The solid-state NMR work was supported by The Netherlands Organization for Scientific Research (Grants 700.26.121 and 700.10.443 to M.B.).

■ REFERENCES

(1) Kataoka, K.; Harada, A.; Nagasaki, Y. *Adv. Drug Delivery Rev.* **2001**, *47*, 113−131.
(2) Torchilin, V. *Pharm. Res.* **2007**, *24*, 1−16.
(3) Talelli, M.; Rijcken, C.; van Nostrum, C.; Storm, G.; Hennink, W. E. *Adv. Drug Delivery Rev.* **2010**, *62*, 231−239.
(4) Miller, T.; Hill, A.; Uezguen, S.; Weigandt, M.; Göpferich, A. *Biomacromolecules* **2012**, *13*, 1707−1718.
(5) Du, J. Z.; Tang, L. Y.; Song, W. J.; Shi, Y.; Wang, J. *Biomacromolecules* **2009**, *10*, 2169−2174.
(6) Gaucher, G.; Marchessault, R. H.; Leroux, J. C. *J. Controlled Release* **2010**, *143*, 2−12.
(7) Sethuraman, V. A.; Bae, Y. H. *J. Controlled Release* **2007**, *118*, 216−224.
(8) Bae, Y.; Jang, W. D.; Nishiyama, N.; Fukushima, S.; Kataoka, K. *Mol. BioSyst.* **2005**, *1*, 242−250.
(9) Oerlemans, C.; Bult, W.; Bos, M.; Storm, G.; Nijsen, J. F. W.; Hennink, W. E. *Pharm. Res.* **2010**, *27*, 2569−2589.
(10) Lammers, T.; Aime, S.; Hennink, W. E.; Storm, G.; Kiessling, F. *Acc. Chem. Res.* **2011**, *10*, 1029−1038.
(11) Yang, R.; Meng, F.; Ma, S.; Huang, F.; Liu, H.; Zhong, Z. *Biomacromolecules* **2011**, *8*, 3047−3055.
(12) Wei, H.; Zhang, X.; Cheng, C.; Cheng, S. X.; Zhuo, R. X. *Biomaterials* **2007**, *28*, 99−107.
(13) Soga, O.; van Nostrum, C. F.; Hennink, W. E. *J. Controlled Release* **2005**, *101*, 383−385.
(14) Censi, R.; Fieten, P. J.; di Martino, P.; Hennink, W. E.; Vermonden, T. *Macromolecules* **2010**, *43*, 5771−5778.
(15) Hsiue, G. H.; Hsu, S.; Yang, C. C.; Lee, S. H.; Yang, I. *Biomaterials* **2002**, *23*, 457−462.
(16) Paasonen, L.; Romberg, B.; Storm, G.; Yliperttula, M.; Urtti, A.; Hennink, W. E. *Bioconjugate Chem.* **2007**, *18*, 2131−2136.

(17) Neradovic, D.; Soga, O.; van Nostrum, C. F.; Hennink, W. E. *Biomaterials* **2004**, *25*, 7491−7498.
(18) Rijcken, C. J.; Snel, C. J.; Schiffelers, R. M.; van Nostrum, C. F.; Hennink, W. E. *Biomaterials* **2007**, *28*, 5581−5593.
(19) Liu, J.; Zeng, F.; Allen, C. *J. Controlled Release* **2005**, *103*, 481−497.
(20) Lo, C. L.; Huang, C. K.; Lin, K. M.; Hsiue, G. H. *Biomaterials* **2007**, *28*, 1225−1235.
(21) Opanasopit, P.; Yokoyama, M.; Watanabe, M.; Kawano, K.; Maitani, Y.; Okano, T. *J. Controlled Release* **2005**, *104*, 313−321.
(22) Joralemon, M. J.; Rachel, K. O. R.; Hawker, C. J.; Wooley, K. L. *J. Am. Chem. Soc.* **2005**, *127*, 16892−16899.
(23) O'Reilly, R. K.; Hawker, C. J.; Wooley, K. L. *Chem. Soc. Rev.* **2006**, *35*, 1068−1083.
(24) Read, E. S.; Armes, S. P. *Chem. Commun.* **2007**, 3021−3035.
(25) van Nostrum, C. F. *Soft Matter* **2011**, *7*, 3246−3259.
(26) Kang, Y.; Taton, T. A. *Angew. Chem., Int. Ed.* **2005**, *117*, 413−416.
(27) Xu, P.; Tang, H.; Li, S.; Ren, J.; van Kirk, E.; Murdoch, W. J.; Radosz, M.; Shen, Y. *Biomacromolecules* **2004**, *5*, 1736−1744.
(28) Chen, H.; Kim, S.; He, W.; Wang, H.; Low, P. S.; Park, K.; Cheng, J. X. *Langmuir* **2008**, *24*, 5213−5217.
(29) Chen, H.; Kim, S.; Li, L.; Wang, S.; Park, K.; Cheng, J. X. *Proc. Natl. Acad. Sci. U.S.A.* **2008**, *105*, 6596−6601.
(30) Talelli, M.; Iman, M.; Varkouhi, A. K.; Rijcken, C. J. F.; Schiffelers, R. M.; Etrych, T.; Ulbrich, K.; van Nostrum, C. F.; Lammers, T.; Storm, G.; Hennink, W. E. *Biomaterials* **2010**, *30*, 7797−7804.
(31) Talelli, M.; Rijcken, C. J. F.; Oliveira, S.; der Meel, R.; Henegouwen, P. M. P.; Lammers, T.; van Nostrum, C. F.; Storm, G.; Hennink, W. E. *J. Controlled Release* **2011**, *1*, 93−102.
(32) Talelli, M.; Oliveira, S.; Rijcken, C. J. F.; Pieters, E. H. E.; Etrych, T.; Ulbrich, K.; van Nostrum, C. F.; Storm, G.; Hennink, W. E.; Lammers, T. *Biomaterials* **2013**, *34*, 1255−1260.
(33) Crielaard, B. J.; Rijcken, C. J. F.; Quan, L.; van der Wal, S.; Altintas, I.; van der Pot, M.; Kruijtzer, J. A. W.; Liskamp, R. M. J.; Schiffelers, R. M.; van Nostrum, C. F.; Hennink, W. E.; Wang, D.; Lammers, T.; Storm, G. *Angew. Chem., Int. Ed.* **2012**, *51*, 7366−7370.
(34) Carstens, M. G.; de Jong, P. H.; van Nostrum, C. F.; Kemmink, J.; Verrijk, R.; de Leede, L. G. J.; Crommelin, D. J. A.; Hennink, W. E. *Eur. J. Pharm. Biopharm.* **2008**, *68*, 596−606.
(35) Yokoyama, M.; Fukushima, S.; Uehara, R.; Okamoto, K.; Sakurai, Y.; Okano, T. *J. Controlled Release* **1998**, *50*, 79−92.
(36) Huh, K. M.; Min, H. S.; Lee, S. C.; Lee, H. J.; Kim, S.; Park, K. *J. Controlled Release* **2008**, *126*, 122−129.
(37) Engelkamp, H.; Middelbeek, S.; JM, R. *Science* **1999**, *284*, 785−788.
(38) Carstens, M. G.; Bevernage, J. J. L.; van Nostrum, C. F.; van Steenbergen, M. J.; Flesch, F. M.; Verrijk, R.; de Leede, L. G. J.; Crommelin, D. J. A.; Hennink, W. E. *Macromolecules* **2007**, *40*, 116−122.
(39) Lee, S. C.; Huh, K. M.; Lee, J.; Cho, Y. W.; Galinsky, R. E.; Park, K. *Biomacromolecules* **2007**, *8*, 202−208.
(40) Yan, J.; Ye, Z.; Chen, M.; Liu, Z.; Xiao, Y.; Zhang, Y.; Zhou, Y.; Tan, W.; Lang, M. *Biomacromolecules* **2011**, *12*, 2562−2572.
(41) Lai, Y.; Long, Y.; Lei, Y.; Deng, X.; He, H.; Sheng, M.; Li, M.; Gu, Z. *J. Drug Targeting* **2012**, *20*, 246−254.
(42) Kim, B. S.; Park, S. W.; Hammond, P. T. *ACS Nano* **2008**, *2*, 386−392.
(43) Kang, N.; Perron, M. È.; Prud'Homme, R. E.; Zhang, Y.; Gaucher, G.; Leroux, J. C. *Nano Lett.* **2005**, *5*, 315−319.
(44) Zhang, J.; Wang, L. Q.; Wang, H.; Tu, K. *Biomacromolecules* **2006**, *7*, 2492−2500.
(45) Etrych, T.; Šubr, V.; Strohalm, J.; Šírová, M.; Říhová, B.; Ulbrich, K. *J. Controlled Release* **2012**, *164*, 346−354.
(46) Neradovic, D.; van Nostrum, C. F.; Hennink, W. E. *Macromolecules* **2001**, *34*, 7589−7591.
(47) Soga, O.; van Nostrum, C.F.; Ramzi, A.; Visser, T.; Soulimani, F.; Frederik, P. M.; Bomans, P. H. H.; Hennink, W. E. *Langmuir* **2004**, *20*, 9388−9395.
(48) Reddy, P. M.; Venkatesu, P. *J. Phys. Chem. B* **2011**, *115*, 4752−4757.
(49) Zhang, Y.; Furyk, S.; Sagle, L. B.; Cho, Y.; Bergbreiter, D. E.; Cremer, P. S. *J. Phys. Chem. C* **2007**, *111*, 8916−8924.
(50) Soga, O.; van Nostrum, C. F.; Hennink, W. E. *Biomacromolecules* **2004**, *5*, 818−821.
(51) Rijcken, C. J. F.; Veldhuis, T. F. J.; Ramzi, A.; Meeldijk, J. D.; van Nostrum, C. F.; Hennink, W. E. *Biomacromolecules* **2005**, *6*, 2343−2351.
(52) Huh, K. M.; Min, H. S.; Lee, S. C.; Lee, H. J.; Kim, S.; Park, K. *J. Controlled Release* **2008**, *126*, 122−129.
(53) Cho, Y. W.; Lee, J.; Lee, S. C.; Huh, K. M.; Park, K. *J. Controlled Release* **2004**, *97*, 249−257.
(54) Jette, K. K.; Law, D.; Schmitt, E. A.; Kwon, G. S. *Pharm. Res.* **2004**, *21*, 1184−1191.
(55) Verweij, J.; Clavel, M.; Chevalier, B. *Ann. Oncol.* **1994**, *5*, 495−505.
(56) Jeener, J.; Meier, B. H.; Bachmann, P.; Ernst, R. R. *J. Chem. Phys.* **1979**, *71*, 4546−4553.
(57) Moad, G.; Rizzardo, E.; Thang, S. H. *Acc. Chem. Res.* **2008**, *41*, 1133−1142.
(58) Braunecker, W. A.; Matyjaszewski, K. *Prog. Polym. Sci.* **2007**, *93*, 93−146.
(59) Jones, M. C.; Leroux, J. C. *Eur. J. Pharm. Biopharm.* **1999**, *48*, 101−111.
(60) Yokoyama, M.; Satoh, A.; Sakurai, Y.; Okano, T.; Matsumura, Y.; Kakizoe, T.; Kataoka, K. *J. Controlled Release* **1998**, *13*, 219−29.
(61) Kwon, G.; Naito, M.; Yokoyama, M.; Okano, T.; Sakurai, Y.; Kataoka, K. *J. Controlled Release* **1997**, *48*, 195−201.
(62) Lee, A. L. Z.; Venkataraman, S.; Sirat, S.; Gao, S.; Hedrick, J. L.; Yang, Y. Y. *Biomaterials* **2011**, *33*, 1921−1928.
(63) Neradovic, D.; van Steenbergen, M.; Vansteelant, L.; Meijer, Y.; van Nostrum, C. F.; Hennink, W. E. *Macromolecules* **2003**, *36*, 7491−7498.
(64) Andrew, E. R.; Bradbury, A.; Eades, R. G. *Nature* **1958**, *182*, 1659−1661.
(65) Schnell, I.; Spiess, H. W. *J. Magn. Reson.* **2001**, *151*, 153−227.
(66) Mafra, L.; Santos, M. S.; Siegel, R.; Alves, I.; Almeida Paz, F. A.; Dudenko, D.; Spiess, H. W. *J. Am. Chem. Soc.* **2011**, *134*, 71−74.
(67) Jeener, J.; Meier, B. H.; Bachmann, P.; Ernst, R. R. *J. Chem. Phys.* **1979**, *71*, 4546−4553.
(68) Baldus, M. *Prog. Nucl. Magn. Reson. Spectrosc.* **2002**, *41*, 1−47.
(69) Lange, A.; Seidel, K.; Verdier, L.; Luca, S.; Baldus, M. *J. Am. Chem. Soc.* **2003**, *125*, 12640−12648.
(70) Ader, C.; Frey, S.; Maas, W.; Schmidt, H. B.; Goerlich, D.; Baldus, M. *Proc. Natl. Acad. Sci. U.S.A.* **2010**, *107*, 6281−6285.
(71) Allix, F.; Curcio, P.; Pham, Q. N.; Pickaert, G.; Jamart-Gregoire, B. *Langmuir* **2010**, *26*, 16818−16827.